# Laser-diode-pumped zigzag slab Nd:YAG master oscillator power amplifier

**Shiguang Li (李世光)[1,2], Xiuhua Ma (马秀华)[1*], Huanhuan Li (李环环)[1,2], Feng Li (李 峰)[1,2], Xiaolei Zhu (朱小磊)[1], and Weibiao Chen (陈卫标)[1]**

[1] *Shanghai Key Laboratory of All Solid-State Laser and Applied Techniques, Research Center of Space Laser Information Technology, Shanghai Institute of Optics and Fine Mechanics, Chinese Academy of Sciences, Shanghai 201800, China*

[2] *University of Chinese Academy of Sciences, Beijing 100049, China*

[*] *Corresponding author: maxiuhua@gmail.com*

Received April 9, 2013; accepted May 13, 2013; posted online July 3, 2013

A high-repetition rate master oscillator power amplifier pumped with laser diodes (LDs) is reported. An injection seeding single-frequency electro-optical $Q$-switched Nd:YAG laser is used as an oscillator, and a conductively cooled Nd:YAG zigzag slab with a bounce-pumped architecture is utilized as a power amplifier. Pulse energies of over 800 mJ at 1 064 nm and 400 mJ at 532 nm, corresponding to average powers of 200 and 100 W, respectively, are achieved with a 12.6-ns pulse width at 250 Hz. Output frequency fluctuations and single-frequency operation are further monitored. Experimental results reveal that the proposed system, which features a single-pass amplified configuration, is a promising design for space-based applications.

*OCIS codes:* 140.3280, 140.3480, 140.3515, 140.3570.
*doi: 10.3788/COL201311.071402.*

Conductively cooled zigzag slabs have been the basis for laser transmitters used in space-based lidar systems [1−3]. Oscillator/amplifier configurations with robust designs, long-term usability, and almost-maintenance-free operation are generally favorablefor flight-worthy and space-qualified lasers[4,5]. However, thermal issues, such as depolarization and aberrations, hindering in the high-power operation of a solid-state amplifier system. Previous studies have developed a laser diode (LD)-pumped solid-state laser with average powers of tens of watts[6], corresponding to 750-mJ pulse energiesat 1 064 nm and diffraction-limited output beams with comparative pulse energiesbased on a master oscillator power amplifier (MOPA)[7] by thermally induced phase distortion of the gain medium. Average output powers of 235[8] and 250 W[9] at pulse repetition frequency (PRF) of 320 and 200 Hz, respectively, have been obtained. Although laser systems with diamond-turned aspheric optics[7], phase-conjugated mirrors[8], and angle-multiplexed ring-type double-pass configurations[9] show excellent performance in the correction of wavefronts and generation of good beam quality with high single-pulse energies, such designs add complexity and volume to prototype systems and increase the difficulty of assembly and calibration. Several components in such systems[10] may also influence all qualification testing procedures, including optical damage and extended lifetime testing, in a complex environment. Compared with conventional rod lasers, zigzag slab lasers[1,2,11,12] have a rectilinear geometry that reduces stress-induced birefringence and an optical path that minimizes thermal- and stress-induced focusing. Thus, zigzag slab lasers are suitable for achieving high average power levels while maintaining good beam quality and polarization contrast. However, slab lasers, especially side-pumped slab lasers, have low laser efficiency, which limits their applications.

Several studies have considered face pumping as an ideal slab design. Face pumping uses the same interface for pumping and cooling, in which the slab is uniformly heated throughout its volume and uniformly cooled through two total-internal-reflection (TIR) faces[13]. However, face-pumped designs typically require direct liquid cooling to satisfy the requirements of uniform pumping and cooling of both faces[14,15]. Direct liquid cooling often damages the slab laser design because it induces slab degradation and the cooling fluid contaminates the slab. Improvement of thermal handling requires the reduction of slab thickness, which, in turn, reduces the pump absorption depth in a face-pumped geometry. The edge-pumped slab design[11] permits symmetric conduction cooling and efficient pump absorption and accepts large numerical aperture pump sources. Alarge aspect ratio (3:1) reduces the robustness of the slab and increases stress, resulting in crystal damage. Conduction cooling[16] features benefits of mechanical stability, protection of the TIR faces, cooling uniformity, and separation of the slab-liquid interface. However, the asymmetries of cooling schemes cause thermal stresses in the crystals that limit their power-scaling potential. The symmetric cooling of edge-pumped slab lasers provides a design that can be scaled to high-power levels.

A MOPA with a PRF of 100 Hz and an output energy of 800 mJ was previously investigated[12]. Given that the signal-to-noise ratio (SNR) of lidar systems is proportional to the square root of the PRF of the laser transmitters under certain single-pulse energies, higher PRFs enable longer detection ranges and higher detection accuracy. Therefore, the PRF of laser transmitters must be increased. We recently successfully developed an injection-seeded single-frequency 1 064-nm laser oscillator with a 250-Hz PRF[17] and high power using a highly efficient conduction cooling technique[18]. In the current

 

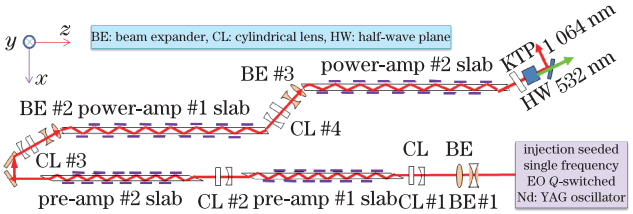


Fig. 1. (Color online) Experimental setup of the single-pass MOPA system

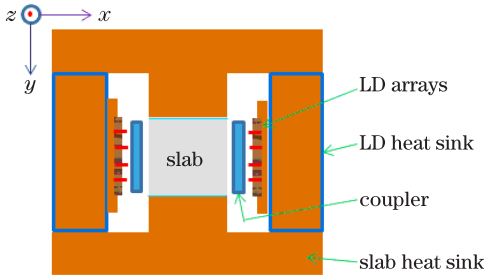


Fig. 2. (Color online) Cross-sectional view of the exit end of LD-pumped laser heads.

works, a single-pass MOPA system was designed to achieve compact and robust output properties at 250-Hz PRF. In this system, a LD-dual-pumped injection seeded single-frequency electro-optical (EO) $Q$-switched Nd:YAG laser was used as the master oscillator. For highly stable PRF operation, the laser crystal was held in a heat sink cooled by a thermo-electric cooler. A negative lens was then inserted into the cavity to compensate for the thermal effect of the rod. The modified ramp-fire technique[17] was implemented to achieve a reliable single longitudinal mode oscillator. In the power amplification stage, a symmetric conductively cooled configuration and zigzag slab design with "pump on bounce" architecture[1,2] were developed to achieve high power, high efficiency, and high single-pulse energy. Second harmonic generation was also successfully developed with a nonlinear potassium titanyl phosphate (KTP) crystal.

The optical layout of the LD-pumped single-frequency MOPA system is illustrated in Fig. 1. The entire setup included one oscillator, two pre-amplifiers, two power-amplifiers, and a second harmonic converter. An injection-seeding single-frequency EO $Q$-switched laser was used as the oscillator. Two quarter-wave plates were inserted at both ends of the composite crystal using a folded standing-wave cavity to eliminate any space-hole burning effect and achieve a compact construction. The approach to cavity length control was based on the modified ramp-fire technique. An adjustable direct current (DC) voltage was introduced to the controlling electronics and applied to the second piezo actuator. Under this servo control unit, the effect of the piezo hysteresis on the frequency stability could be sufficiently eliminated. A smooth temporal pulse profile and high-energy stability output were achieved, and these could largely reduce the occurrence of optical damage stemming from the amplification of amplitude modulations in the laser pulse. The output beam was steered toward the amplifiers.

The application of lasers in space imposes a unique set of requirements on the gain media and the thermo-mechanical structures that hold them for both oscillators and amplifiers. Two of the highest priority requirements include 1) optimization of the gain media design for efficiency and 2) high conductivity of the thermal interface to the gain medium and its supporting structure (i.e., no direct liquid cooling). Two identical Nd:YAG zigzag slabs (5×5×110 (mm)) with the Brewster angle design were combined ina pump-on-bounce approach[3] in the pre-amp stage to maximize the extraction efficiency and minimize diffraction effects. The input and output beams were parallel to the principal slab axis, and the angle of incidence of these beams was near the Brewster angle. The pump arrays were grouped in pairs at the bounce points rather than uniformly along the slab, as shown in Fig. 1. Considering the diffraction at the slab edges, a larger input beam was used during testing but without compromising beam quality degradation. The maximum input should be used in the power-amplifier stage to optimize the extraction of the amplifiers. Two identical slabs with larger dimensions (8×8×120 (mm)) were cut for near-normal incidence at 48° relative to the $\boldsymbol{x}$ direction, corresponding to an internal zigzag angle of approximately 40°. The aspect ratio (1:1) of the slab was selected to increase the robustness of the slab and prevent the crystal from breaking. Crystals with $Nd^{3+}$ concentration of 1% were coated with an antireflection (AR) film at 808 nm on the TIR surface. The peak power of the LD arrays was 12 kW for pumping of the pre-amplifiers and 15 kW for the power-amplifiers with a pulse duration of 200 $\mu$s (duty factor of 5%).

The conductively cooling architecture of the current study was based on pumping from two opposite sides ($\boldsymbol{x}$

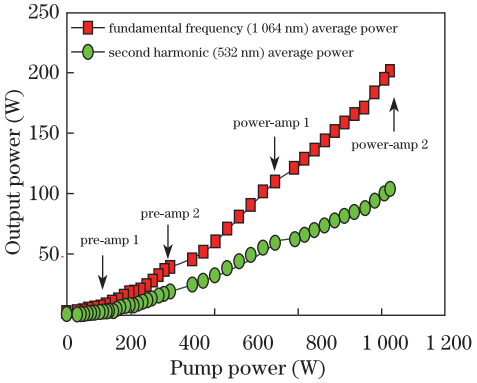


Fig. 3. (Color online) Output average power versus pump power and the power value after each amplified stage.

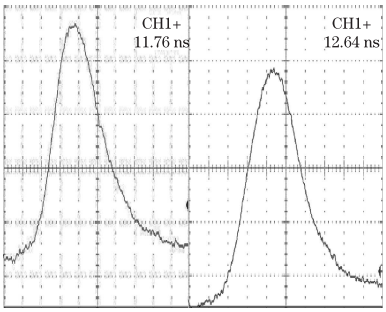


Fig. 4. Laser pulse shape from the oscillator (left) and the MOPA (right).

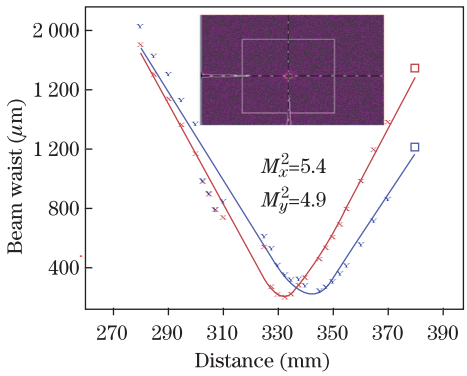


Fig. 5. (Color online) Beam quality of the MOPA (250 Hz, 800 mJ per pulse energy). Inset: beam profile at the far field.

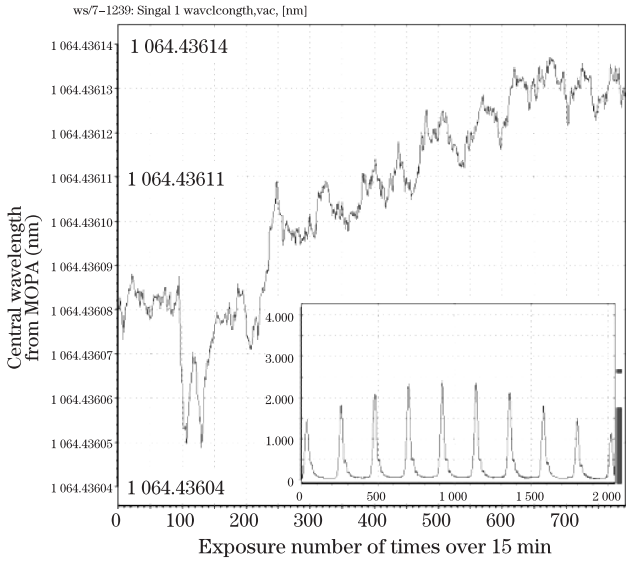


Fig. 6. (Color online) Shot-to-shot time record of the wavelengths obtained from the MOPA. Inset: single frequency operation.

direction) in the TIR plane and cooling in the perpendicular plane (***y*** direction), as shown in Fig. 2. For high PRF operation, temperature gradients in the gain material as a result of heating can lead to stress fracture, and the output beam quality is adversely affected by thermal lensing and birefringence below the stress fracture limit. The uniformity of the pump beam[1] in the amplifier stage is considerably important in decreasing the thermal gradient and achieving good beam quality. For the output beams from the LD arrays, the divergence angle in the slow axis is much smaller than that in the fast axis. Thus, couplers (rectangular waveguide, 5×5×120 (mm)) were inserted between the pump LD arrays, and the gain medium for fast axis shaping consequently increased the pump uniformity. Indium foils of 0.05-mm thickness were placed between the slabs and the copper heat sink to ensure sufficiently close contact and uniform thermal conduction and effectively alleviate mechanical stress. Due to its high damage threshold and high nonlinear coefficient, a KTP crystal was used for the efficient generation of the second harmonic.

The oscillator produces 10-mJ pulse energy and near-Gaussian 11-ns pulse duration at a 250-Hz pulse repetition frequency[17]. The output beam was measured at it $M_x^2$=1.19 and $M_y^2$=1.22, which serve as an excellent reference for the MOPA. The thermal lensing effect is very important in the amplifier; thus, the thermal lensing compensation was meticulously measured and constructed to obtain a high-beam quality laser. The measured values range from 30 to 60 cm and are unequal in the ***x*** and ***y*** directions. Cylindrical lenses were explored for thermal aberration correction[18].

Figure 3 shows the measured average output power of fundamental frequency and second harmonic from the MOPA as a function of the LD average pump power at 250-Hz operation, as well as the power value after each amplification stage. The output pulse power initially increases exponentially with the pump power and then increases nearly linearly as the amplifier is sufficiently extracted and saturated. Maximal output powers of over 200 (fundamental) and 100 (double frequency) W are achieved, and the corresponding single pulse energies are 800 and 400 mJ, respectively. The frequency-doubling efficiency is near 50%. The degree of polarization was also measured using a Glan prism, and a value of 99.2% is obtained on the basis of the measured results with 800-mJ single-pulse energy at 1 064 nm. The high degree of polarization of the pulse laser achieves high-efficiency nonlinear frequency conversion. An optical-optical efficiency of 19% and EO efficiency of 9% are also achieved by the master oscillator.

Laser pulses from the oscillator and MOPA system were then recorded. The pulse duration of the oscillator is 11.76 ns, as shown in Fig. 4. Note that the leading edge of the pulse shows higher gain during amplification; thus, the leading edge becomes sharper after amplification. This phenomenon occurs in the preampstage, and the pulse width is shorter than that of the oscillator (pre-amp 1, 10.2 ns; pre-amp 2, 9.5 ns). However, the leading edge of the pulse becomes slower with linear magnificationbecause of saturation gain during the power-ampstage[12]. Therefore, the amplified pulse from the MOPA is slightly stretched to 12.6 ns, as seen in Fig. 4. The highest peak power obtained is 71.4 MW, which indicates that the present MOPA system has good temporal fidelity. The output beam quality was measured by a laser beam analyzer ($M^2$-200, Ophir-Spiricon, USA) and $M^2$ values of 5.4 and 4.9 are obtained in the ***x*** and ***y*** directions, respectively. The measurement results are shown in Fig. 5; the inset in the figure shows the beam profile at the far field.

A fiber-coupled wave meter (WS-7, High Finesse, Germany) running in a shot-by-shot mode was used to monitor the laser wavelength. The measurement results are presented in Fig. 6. A frequency fluctuation of 23.8 MHz is obtained from the MOPA system after operation for over 15 min, and the corresponding wavelengths range from 1 064.43605 to 1 064.43614 nm. Within the same period, the frequency fluctuation of the oscillator is measured to be ∼21.2 MHz. The frequency fluctuation from MOPA is larger than that from the oscillator, presumably because of the lower temperature control accuracy of the LD pump for MOPA. The line width of the MOPA was calculated, and the value obtained is always less than 100 MHz, which is the limit of the proposed instrument. The output of the single-frequency operation of the MOPA was qualitatively recorded by the long

Fizeau interferometer of the wave meter, as shown in the inset of Fig. 6. The current design clearly hardly influences the single-frequency output characteristics even at higher single-pulse energies.

In conclusion, a LD-pumped MOPA system with high average power and high energy at 250 Hz PRF is developed. The system achieves stable single-frequency operation with good temporal fidelity after amplification. Single pulse energies of 800 mJ (1 064 nm) and 400 mJ (532 nm) are successfully obtained at a pulse width of 12.6 ns with an optical-to-optical conversion efficiency of 19% (808 to 1 064 nm) using the pump-on-bounce architecture and experimentally optimized thermal lens compensation system. The single-frequency high-energy laser system and its nonlinear conversion are expected to become powerful sources for the measurement and investigation of the global carbon cycle using active remote sensing from space[19].

## References


1. F. E. Hovis, N. Martin, and R. Burnham, Proc. SPIE **5798,** 101 (2005).
2. N. S. Prasad, U. N. Singh, and F. Hovis, in *Proceedings of Earth Science Technology Conference (ESTC)* **6,** (2006).
3. J. Wang, L. Yin, X. Shi, X. Ma, L. Li, and X. Zhu, Chin. Opt. Lett. **8,** 591 (2010).
4. R. Zhu, J. Wang, J. Zhou, J. Liu, and W. Chen, Chin. Opt. Lett. **10,** 091402 (2012).
5. J. Xu, R. Su, H. Xiao, P. Zhou, and J. Hou, Chin. Opt. Lett. **10,** 031402 (2012).
6. J. J. Kasinski, W. Hughes, D. Dibiase, P. Bournes, and R. Burn ham, IEEE J. Quantum Electron. **28,** 977 (1992).
7. J. J. Kasinski and R. L. Burnham, Appl. Opt. **35,** 5949 (1996).
8. S. Amano and T. Mochizuki, IEEE J. Quantum Electron. **37,** 296 (2001).
9. K. Tei, M. Kato, Y. Niwa, S. Harayama, Y. Maruyama, T. Matoba, and T. Arisawa, Opt. Lett. **23,** 514 (1998).
10. C. Basu, P. Wessels, J. Neumann, and D. Kracht, Opt. Lett. **37,** 2862 (2012).
11. T. S. Rutherford, W. M. Tulloch, S. Sinha, and R. L. Byer, Opt. Lett. **26,** 986 (2001).
12. X. Ma, J. Wang, J. Zhou, X. Zhu, and W. Chen, Appl. Phys. B **103,** 809 (2011).
13. T. J. Kane, J. M. Eggleston, and R. L. Byer, IEEE J. Quantum Electron. **21,** 1195 (1985).
14. J. M. Eggleston, T. J. Kane, K. Kuhn, J. Unternahrer, and R. L. Byer, IEEE J. Quantum Electron. **20,** 289 (1984).
15. D. Mudge, P. J. Veitch, J. Munch, D. Ottaway, and M. W. Hamilton, IEEE J. Sel. Top. Quantum **3,** 19 (1997).
16. J. P. Chernoch, "Laser cooling method and apparatus", U. S. Patent 3679999 (1972).
17. J. Wang, R. Zhu, J. Zhou, H. Zang, X. Zhu, and W. Chen, Chin. Opt. Lett. **9,** 081405 (2011).
18. H. Li, S. Li, X. Ma, J. Wang, and X. Zhu, Chinese J. Lasers (in Chinese) **39,** 0302008 (2012).
19. S. Li, H. Li, X. Ma, J. Wang, X. Zhu, and W. Chen, Infrared Laser Eng. (in Chinese) **41,** 3249 (2012).